

011

THEORETICAL INVESTIGATION OF THE  $(\text{H}_2\text{I}_2)$   
POTENTIAL ENERGY SURFACE

By

LEWIS E. STIVERS,

Bachelor of Science

University of Tulsa

Tulsa, Oklahoma

1965

March 9, 70

Submitted to the Faculty of the Graduate College  
of the Oklahoma State University  
in partial fulfillment of the requirements  
for the Degree of  
MASTER OF SCIENCE  
May, 1968

10-10-68  
10-10-68  
10-10-68

CONFIDENTIAL - SECURITY INFORMATION  
NOV 10 1968

Thesis  
1968  
Secret  
10-10-68

CONFIDENTIAL - SECURITY INFORMATION  
NOV 10 1968  
CONFIDENTIAL - SECURITY INFORMATION  
NOV 10 1968  
CONFIDENTIAL - SECURITY INFORMATION  
NOV 10 1968

CONFIDENTIAL - SECURITY INFORMATION  
NOV 10 1968  
CONFIDENTIAL - SECURITY INFORMATION  
NOV 10 1968  
CONFIDENTIAL - SECURITY INFORMATION  
NOV 10 1968

OKLAHOMA  
STATE UNIVERSITY  
LIBRARY  
OCT 27 1968

THEORETICAL INVESTIGATION OF THE  $(\text{H}_2\text{I}_2)$   
POTENTIAL ENERGY SURFACE

Thesis Approved:

Leonid M. Raff  
Thesis Adviser  
Robert D. Freeman  
H. Durham  
Dean of the Graduate College

688766

## ACKNOWLEDGEMENTS

I am deeply indebted to Dr. Lionel M. Raff for his patience and guidance throughout this project. His invaluable advice and interest in this problem were of inestimable value. My wife, Joan, deserves credit for her patience, understanding, and encouragement.

I wish to thank the Oklahoma State University Computing Center for use of their facilities in preparation of this thesis.

My parents deserve much credit for their patience and support throughout this study.

Acknowledgement is also due to Mrs. Karol Roberts for her excellent typing of this thesis.

TABLE OF CONTENTS

Chapter	Page
I. INTRODUCTION. . . . .	1
Absolute Reaction Rate Theory. . . . .	2
Classical Trajectory Analysis. . . . .	4
II. MULTI-BODY POTENTIAL ENERGY SURFACES. . . . .	6
Eyring H <sub>3</sub> Surface. . . . .	6
Eyring-Sato H <sub>3</sub> Surface . . . . .	7
Porter and Karplus H <sub>3</sub> Surface. . . . .	8
Conroy H <sub>3</sub> Surface. . . . .	8
Karplus, Pederson and Morokuma H <sub>4</sub> Surface. . . . .	9
III. (H <sub>2</sub> I <sub>2</sub> ) SEMIEMPIRICAL POTENTIAL SURFACE. . . . .	10
IV. RESULTS AND DISCUSSION. . . . .	20
V. SUMMARY AND CONCLUSIONS . . . . .	32
BIBLIOGRAPHY . . . . .	34

## LIST OF TABLES

Table	Page
I. Constants for Calculation of ${}^3E$ . . . . .	20
II. Uncorrected ${}^3E_{H_2}$ From Equation (54). . . . .	22
III. Corrected ${}^3E$ for HI and $I_2$ . . . . .	23
IV. Singlet and Triplet State Morse Parameters . . . . .	23

## LIST OF FIGURES

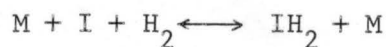
Figure	Page
1. Regular, Planar Trapezoidal Configuration . . . . .	24
2. Distorted, Planar Trapezoidal Configuration . . . . .	25
3. Out-of-Plane Configuration. . . . .	26
4. Perpendicular Configuration . . . . .	27
5. Linear Configuration. . . . .	28

## CHAPTER I

### INTRODUCTION

Recently, considerable interest has been raised in the mechanism of the reaction of hydrogen and iodine. Bodenstein<sup>1</sup> reported experimental results in 1899 and interpreted these results as evidence of second-order reaction of type I, that is, first-order with respect to both hydrogen and iodine. In 1928, Kistiakowsky<sup>2</sup> reported that the rate of decomposition of hydrogen iodide was bimolecular. The reaction of hydrogen and iodine was quickly adopted as an example of a second-order reaction, type I.

Many studies have been made on the ( $\text{H}_2\text{I}_2$ ) system. A photochemical experiment was reported by Sullivan<sup>3</sup> in 1967. In this experiment, Sullivan measured the reaction rate with photochemically produced iodine atoms at temperatures low enough to prevent thermal reaction interference. The Arrhenius parameters of the photochemical reaction matched the Arrhenius parameters of the high temperature data. A termolecular mechanism, that is the reaction of hydrogen and two iodine atoms, was one of two mechanisms proposed by Sullivan. The other was a two-step process in which the second step is the rate-determining one.



Difficulties arise in kinetic work when the data is analyzed. It is very difficult to determine when iodine atoms are present since any collision of iodine atoms on a sensor surface yields iodine molecules. No experimental work has been able to prove the mechanism of the reaction.

Noyes<sup>4</sup> has reported on the apparent paradox of the hydrogen iodide reaction. Sullivan's work has led to the conclusion that the reaction is exclusively termolecular. However, the intermediate or activated complex in the reaction should be able to be approached by either iodine atoms or molecules and through this reasoning, Absolute Reaction Rate Theory<sup>5</sup> predicts that Sullivan's rate of termolecular reaction should be less than the combined reaction rate at high temperature.

Theoretical techniques, such as absolute rate theory and classical trajectory analysis, might be able to shed light on the difficulties presented by experimental work. These theories are reviewed in the next section.

### Absolute Reaction Rate Theory

For an atomic or molecular process which requires an activation energy, that is, one in which a minimum amount of energy must be supplied to the reactants in order to cause reaction, the atoms or molecules must approach each other to form an activated complex. The activated complex may be pictured as sitting atop a barrier between the reactants and products. The rate of the reaction is given as the velocity of the activated complex travelling over the top of the barrier. In this theory, the activated complex is treated as a molecule that is stable in all respects except for the normal vibrational frequency in



the coordinate of decomposition. By making the assumptions that the initial reactants are always in equilibrium with the activated complex and that the activated complex decomposes at a definite rate, the following expression for the rate of reaction,  $k$ , may be written<sup>5</sup>:

$$k = K \frac{k' T}{h} \cdot \frac{F^\ddagger}{F_A F_B \dots} e^{-E_0/RT} \quad (1)$$

In this equation,  $T$  is the absolute temperature;  $R$  is the gas constant;  $E_0$  is the difference in the zero-point vibrational energy of the reactants and that of the activated complex;  $F_A, F_B, \dots$  etc. are the partition functions of the reactants  $A, B, \dots$  etc. respectively;  $F^\ddagger$  is the partition function of the activated complex;  $h$  is planck's constant;  $k'$  is Boltzmann's constant; and  $K$  is the transmission coefficient.

Another form of the rate equation is:

$$k = K \frac{k' T}{h} K^\ddagger \quad (2)$$

In this equation  $K^\ddagger$  is the equilibrium constant expression between the activated complex and the reactants. If one makes the usual substitutions for the equilibrium constant, the rate expression becomes<sup>5</sup>:

$$k = K \frac{k' T}{h} e^{(\Delta S^\ddagger)/R} e^{-(\Delta H^\ddagger)/RT} \quad (3)$$

where  $(\Delta S^\ddagger)$  is the entropy of activation and  $(\Delta H^\ddagger)$  is the enthalpy of activation.

A quantitative calculation cannot be made using equation (3) since the entropy of activation of the activated complex is not attainable.

However, equation (2) may be used providing the equilibrium constant is evaluated. This evaluation is possible if the partition functions of the reactants are known and the partition function of the activated complex is calculated from the frequency of the normal modes of vibration and the geometry of the activated complex. These quantities are attainable if the potential energy surface of the system is known.

### Classical Trajectory Analysis

A new form of kinetic study has been developed in the last few years<sup>6</sup>. This form of analysis, known as Classical Trajectory Analysis, involves the assumption that classical mechanics describes the system. To begin with, the molecules or atoms are separated at a distance sufficiently large so as to ensure a small interaction potential. The equations of motion are then integrated until there has been a reaction or all chance of a reaction is past. This procedure is called a trajectory calculation. For a detailed study of a system, many such calculations must be made to allow proper averaging over initial conditions. In this manner, it is possible to relate the theoretical analysis with experimental work. If, in an actual experiment, a given set of initial conditions could be defined exactly, an averaging technique would not be necessary.

The equations of motion referred to above may be expressed as:

$$\dot{Q}_i = \frac{\partial H}{\partial P_i} \quad \text{and} \quad \dot{P}_i = - \frac{\partial H}{\partial Q_i} \quad (4)$$

where  $Q_i$  is a generalized coordinate,  $H$  the Hamiltonian and  $P_i$  a generalized momentum, conjugate to  $Q_i$ . By expressing the Hamiltonian

as the sum of the kinetic energy,  $T$ , and the potential energy  $V$ , the equations of motion may be written as:

$$\dot{Q}_i = \frac{\partial T}{\partial P_i} \quad \text{and} \quad \dot{P}_i = - \frac{\partial V}{\partial Q_i} \quad (5)$$

providing  $V$  is a function of particle position only.

Following the assumption that classical mechanics is sufficient to describe the system, the kinetic energy term may be obtained analytically. For a trajectory to be calculated, however, a potential energy function is again required.

Although an exact quantum mechanical formulation of the ( $H_2I_2$ ) system potential is not possible at the present time, several semiempirical methods<sup>5, 7-15</sup> have been employed with varying degrees of success for other systems.

## CHAPTER II

### MULTI-BODY POTENTIAL ENERGY SURFACES

#### Eyring H<sub>3</sub> Surface

One of the earliest attempts to obtain a potential energy surface for a system was made by Eyring<sup>5</sup>. In 1936, Eyring reported a semi-empirical method of analysis of the H<sub>3</sub> system. In this analysis, the potential energy function was taken to be the lowest root of

$$E = D + n(W_{ab} + W_{bc} + W_{ac}) \\ + (1-n)(W_{ab}^2 + W_{bc}^2 + W_{ac}^2 - W_{ab}W_{bc} \\ - W_{ab}W_{ac} - W_{bc}W_{ac})^{\frac{1}{2}}, \quad (6)$$

where D is the heat of dissociation of H<sub>2</sub> minus the half-quanta of zero-point energy; W<sub>ab</sub> is the energy of H<sub>2</sub> for the internuclear separation r<sub>ab</sub> and similarly for W<sub>bc</sub> and W<sub>ac</sub>; and n is the fraction of the sum of the binding energy of H<sub>2</sub> for the given internuclear distances.

A potential contour map of this surface for the linear configuration for H<sub>3</sub> shows that a basin is formed at the saddle point. Such a result indicates that as the reactants follow the reaction coordinate, they first pass over a barrier, then fall into a potential energy well as a metastable activated complex. Other attempts to generate the H<sub>3</sub> surface have failed to yield such a basin along the reaction coordinate.

Eyring-Sato H<sub>3</sub> Surface

In 1954, Sato<sup>7</sup> reported on his work with the H<sub>3</sub> system. For the potential energy of two atoms close together and the third at infinity, Sato used the Heitler-London<sup>16</sup> results for the energy of the bonding and the antibonding cases. The energy of the bonding case was given as the Morse function:

$$E_{\text{bond}} = D_e \left[ e^{-2\beta(r-r_e)} - 2e^{-\beta(r-r_e)} \right] \quad (7)$$

where  $E_{\text{bond}}$  is the energy of the bonding state;  $D_e$  is the dissociation energy of H<sub>2</sub>;  $\beta$  is a constant;  $r_e$  is the equilibrium bond distance of H<sub>2</sub>; and  $r$  is the bond length of H<sub>2</sub>.

For the energy of the antibonding state, Sato proposed the following expression:

$$E_{\text{Anti}} = \frac{D_e}{2} \left[ e^{-2\beta(r-r_e)} + 2e^{-\beta(r-r_e)} \right] \quad (8)$$

This fits the calculated data for the  $\sum^3$  u state of H<sub>2</sub> reasonably well. By using assumptions similar to those of London<sup>17</sup>, Sato<sup>7</sup> derived the potential energy equation:

$$E = \frac{1}{1+k} \left[ Q_{AB} + Q_{AC} + Q_{BC} - \left\{ \frac{1}{2} \left[ (\alpha_{AB} - \alpha_{BC})^2 + (\alpha_{BC} - \alpha_{CA})^2 + (\alpha_{CA} - \alpha_{AB})^2 \right] \right\}^{\frac{1}{2}} \right] \quad (9)$$

where  $k$  corresponds to the square of overlap integral while  $Q_{ij}$  and  $\alpha_{ij}$  represent coulomb and exchange integrals respectively between

centers  $i$  and  $j$ . The only difference between this result and London's is the presence of the constant  $k$ . In the range of large  $r$ ,  $k$  approaches zero and the two results are the same.

The potential energy plot obtained by this method differs from that of Eyring's attempt in that it does not have a basin, but instead the expected reaction barrier.

#### Porter and Karplus $H_3$ Surface

Recently, Porter and Karplus<sup>8</sup> have reported results obtained for the  $H_3$  system. Previous attempts had either neglected overlap or treated it as an empirical parameter. In this work, all overlap and multiple-exchange integrals are included. These integrals are estimated through various semiempirical procedures<sup>8</sup>. Agreement is found to be quite good for a comparison of the experimental activation energy and the activation energy calculated using this surface in a Classical Trajectory Analysis<sup>8</sup>. This work also agrees with the prediction of the linear complex as the least energetic.

#### Conroy $H_3$ Surface

Conroy<sup>9-14</sup> has recently reported a rigorous solution of the  $H_3$  system. The calculations reported include both symmetric and unsymmetric linear systems.

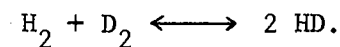
In these calculations, Conroy employed single-centered basis functions constructed so as to produce the correct behavior at the nuclei and as the interelectronic distance,  $r_{ij}$ , approached zero. These functions were incorporated into a variance minimization scheme in which integrals were evaluated by Monte Carlo techniques. Final energy

values were obtained via the variation formula and an extrapolation scheme to zero variance.

By comparing the Conroy surface obtained with the semiempirical surface of Porter and Karplus<sup>8</sup>, one sees that agreement is very good. This agreement lends weight to the validity of the semiempirical methods used by Porter and Karplus to evaluate the overlap and the multiple exchange integrals.

#### Karplus, Pederson and Morokuma H<sub>4</sub> Surface

Work on the H<sub>4</sub> system was reported in 1967<sup>15</sup>. An approximate surface was obtained by a semiempirical method of the London-Eyring-Sato type. Although the surface obtained by this method was too high at the saddle point, it was used in a quasi-classical trajectory study of the reaction:



### CHAPTER III

#### (H<sub>2</sub>I<sub>2</sub>) SEMIEMPIRICAL POTENTIAL SURFACE

In order to carry out a theoretical analysis of the (H<sub>2</sub>I<sub>2</sub>) system by either absolute reaction rate theory or classical trajectory analysis, a potential energy surface is required. Although a rigorous treatment of the (H<sub>2</sub>I<sub>2</sub>) system is, at the present time, impossible, various semi-empirical methods are available with which to construct a potential energy surface. Several of these methods are reviewed in the previous chapter. With such methods, a representation of the (H<sub>2</sub>I<sub>2</sub>) surface has been formulated.

By using the London<sup>17</sup> formulation, the potential energy is obtained as a function of the coulombic and exchange integrals of the system:

$$V = Q - \left[ \frac{1}{2} \left\{ (\alpha_1 - \alpha_2)^2 + (\alpha_2 - \alpha_3)^2 + (\alpha_3 - \alpha_1)^2 \right\} \right]^{\frac{1}{2}} \quad (10)$$

where  $Q = Q_{AB} + Q_{AC} + Q_{AD} + Q_{BC} + Q_{BD} + Q_{CD}$ ,  $\alpha_1 = \alpha_{AB} + \alpha_{CD}$ ,  $\alpha_2 = \alpha_{AD}$

$$+ \alpha_{BC} \text{ and } \alpha_3 = \alpha_{AC} + \alpha_{BD}.$$

These integrals may be approximated through the use of the Heitler-London<sup>16</sup> expression for the singlet state and triplet state energies of a molecule:

$$E_{AB} = \frac{Q_{AB} + \alpha_{AB}}{1 + S_{AB}^2} \text{ and } {}^3E_{AB} = \frac{Q_{AB} - \alpha_{AB}}{1 - S_{AB}^2} \quad (11)$$



If one neglects the overlap integral of equation (11), then that equation becomes:

$$E_{AB} = Q_{AB} + \alpha_{AB} \text{ and } {}^3E_{AB} = Q_{AB} - \alpha_{AB} . \quad (12)$$

Solving for the coulombic and exchange integrals gives the result:

$$Q_{AB} = \frac{E_{AB} + {}^3E_{AB}}{2} \text{ and } \alpha_{AB} = \frac{E_{AB} - {}^3E_{AB}}{2} . \quad (13)$$

The singlet state energies for the molecules in question present no problem. The potential function proposed by Morse<sup>18</sup> is used for the singlet state energy.

$$E = {}^1D_e \left[ e^{-2\beta(r - r_e)} - 2e^{-\beta(r - r_e)} \right] , \quad (14)$$

where  ${}^1D_e$  is the dissociation energy,  $\beta$  is a constant related to the ground state vibrational frequency, and  $r_e$  is the equilibrium bond length. The constant  $\beta$  is given by:

$$\beta = 2\pi\nu_0 \sqrt{\frac{\mu}{2D_e}} \quad (15)$$

where  $\nu_0$  is the ground state vibrational frequency and  $\mu$  is the reduced mass.

To represent the triplet state,  ${}^3E$ , Porter and Karplus<sup>8</sup> have proposed a modification of the Morse function,

$${}^3E = {}^3D_e \left[ e^{-2\beta(r - r_e)} + 2e^{-\beta(r - r_e)} \right] . \quad (16)$$

In this form  ${}^3\text{De}$  and  ${}^3\beta$  are adjustable parameters used to fit the triplet state energy curve for the system.

For the  $\text{H}_2$  system, Kolos and Roothaan<sup>19</sup> have carried out accurate quantum calculations to obtain a representation of the lowest triplet state for the system. Equation (16) has been shown<sup>8</sup> to fit this data quite accurately.

In this work, Equation (16) has been employed to obtain a representation for the triplet state energy of the HI and  $\text{I}_2$  systems. However, since no data for the triplet state energies of HI and  $\text{I}_2$  are available, it has been necessary to carry out semiempirical calculations to obtain approximate values for these energies.

For the diatomic molecule AB separated by distance R, a semiempirical molecular orbital approach, in which the molecule is treated as a two-electron system with nonpolarizable cores, has been employed to obtain the triplet state energies. Wave functions were represented by a single Slater determinant in which the molecular orbitals were constructed from a minimal basis set; that is, one atomic orbital centered on each of the two nuclei:

$$\psi = \frac{1}{\sqrt{2}} \begin{vmatrix} \lambda_1(1) & \lambda_1(2) \\ \lambda_2(1) & \lambda_2(2) \end{vmatrix} \quad (17)$$

where

$$\lambda_1 = [c_1 \phi_A + c_2 \phi_B] \alpha$$

$$\lambda_2 = [c_3 \phi_A + c_4 \phi_B] \alpha$$

$\alpha$  is the spin function and  $\phi_A(1)$  is the atomic orbital of electron 1 centered on atom A. The atomic orbitals used were Slater orbitals.

For hydrogen, a 1 s orbital was used, for iodine, the 5 p $\sigma$  orbital was employed for the bonding electron and the remaining 52 electrons were treated as part of the nonpolarized core and assumed not to take part in the bonding. When equation (17) is expanded, the wave function takes the form:

$${}^3\Psi = K[\phi_A(1)\phi_B(2) - \phi_A(2)\phi_B(1)] \quad (18)$$

where

$$K = \frac{1}{\sqrt{2 - 2S_{AB}^2}} \quad (19)$$

where  $S_{AB}$  represents the overlap integral, i.e.

$$S_{AB} = \langle \phi_A | \phi_B \rangle \quad (20)$$

Ignoring nuclear repulsion energy and writing the Hamiltonian for the AB system in atomic units, one obtains

$$\begin{aligned} \mathcal{H} = & -\frac{1}{2} \nabla_1^2 - \frac{1}{2} \nabla_2^2 + \frac{1}{r_{12}} - V_A(1) - V_A(2) \\ & - V_B(1) - V_B(2), \quad (21) \end{aligned}$$

where  $V_A(1)$  is the potential seen by electron 1 due to the presence of core A.

When the wave function and Hamiltonian are substituted into the electronic energy equation

$${}^3E_e = \int {}^3\Psi \mathcal{H} {}^3\Psi d\tau, \quad (22)$$

the expanded equation is of the form

$${}^3E_e = \frac{1}{(1 - S_{AB}^2)} [X_1 - X_2], \quad (23)$$

where 
$$X_1 = \langle \phi_A(1) \phi_B(2) | \mathcal{H} | \phi_A(1) \phi_B(2) \rangle \quad (24)$$

and 
$$X_2 = \langle \phi_A(1) \phi_B(2) | \mathcal{H} | \phi_A(2) \phi_B(1) \rangle . \quad (25)$$

The integrals of equations (24) and (25) may be divided into various forms by separating the Hamiltonian as follows:

$$\mathcal{H} = \mathcal{H}_A + \mathcal{H}_B + \mathcal{H}_{INT} \quad (26)$$

where 
$$\mathcal{H}_A = -\frac{1}{2} \nabla_1^2 - V_A(1), \quad (27)$$

$$\mathcal{H}_B = -\frac{1}{2} \nabla_2^2 - V_B(2), \quad (28)$$

and 
$$\mathcal{H}_{INT} = \frac{1}{r_{12}} - V_A(2) - V_B(1) . \quad (29)$$

Substitution of equations (26)-(29) into equations (24) and (25) will yield the following types of integrals:

$$\langle \phi_A(1) \phi_B(2) | \mathcal{H}_A | \phi_A(1) \phi_B(2) \rangle \quad (30)$$

$$\langle \phi_A(1) \phi_B(2) | \frac{1}{r_{12}} | \phi_A(1) \phi_B(2) \rangle \quad (31)$$

$$\langle \phi_A(1) \phi_B(2) | V_A(2) | \phi_A(1) \phi_B(2) \rangle \quad (32)$$

$$\langle \phi_A(1) \phi_B(2) | \mathcal{H}_A | \phi_A(2) \phi_B(1) \rangle \quad (33)$$

$$\left\langle \phi_A(1)\phi_B(2) \left| \frac{1}{r_{12}} \right| \phi_A(2)\phi_B(1) \right\rangle \quad (34)$$

$$\left\langle \phi_A(1)\phi_B(2) \left| V_A(2) \right| \phi_A(2)\phi_B(1) \right\rangle \quad (35)$$

These integrals have been evaluated using various semiempirical approximations. The integral of equation (30) is approximated as

$$\left\langle \phi_A(1)\phi_B(2) \left| \mathcal{H}_A \right| \phi_A(1)\phi_B(2) \right\rangle = -I_A \quad (36)$$

where  $I_A$  is the ionization potential of atom A. This procedure in essence assumes that  $\phi_A$  represents an exact eigenfunction of  $\mathcal{H}_A$  whose associated energy is the experimental ionization potential. A similar approximation has been made by Pohl<sup>20</sup> and by Pohl and Raff<sup>21</sup> to treat the hydrogen halides and interhalogen systems. Integral (33) is evaluated in a similar manner.

The two-electron integrals of equation (31) are evaluated with Pople's<sup>22</sup> approximation:

$$\left\langle \phi_A(1)\phi_B(2) \left| \frac{1}{r_{12}} \right| \phi_A(1)\phi_B(2) \right\rangle = R_{12}^{-1} \quad (37)$$

where  $R_{12}$  is the distance between nuclei.

Integral (32) is also evaluated by Pople's approximation:

$$\left\langle \phi_A(1)\phi_B(2) \left| V_A(2) \right| \phi_A(1)\phi_B(2) \right\rangle = R_{12}^{-1} \quad (38)$$

By expansion and use of the above evaluation schemes,  $X_1$  becomes:

$$X_1 = -I_A - I_B - R_{12}^{-1} \quad (39)$$

In addition to the integrals in  $X_1$ ,  $X_2$  includes:

$$\langle \phi_A(1) \phi_B(2) \left| \frac{1}{r_{12}} \right| \phi_A(2) \phi_B(1) \rangle = \frac{S_{AB}^2}{4} \left[ 2R_{12}^{-1} + I_A + I_B + A_A + A_B \right], \quad (40)$$

where  $A_A$  is the electron affinity of atom A. This evaluation is made using Mulliken's<sup>23</sup>, Pariser's<sup>24</sup> and Pople's<sup>22</sup> approximations. The first of these changes the integral in equation (34) into

$$\frac{S_{AB}^2}{4} \langle \phi_A^2(1) + \phi_B^2(1) \left| \frac{1}{r_{12}} \right| \phi_A^2(2) + \phi_B^2(2) \rangle. \quad (41)$$

This yields four integrals that may be evaluated by Pople's<sup>22</sup> and Pariser's<sup>24</sup> approximations: i.e.

$$\langle \phi_A^2(1) \left| \frac{1}{r_{12}} \right| \phi_B^2(2) \rangle = R_{12}^{-1} \quad (42)$$

and

$$\langle \phi_B^2(1) \left| \frac{1}{r_{12}} \right| \phi_A^2(2) \rangle = R_{12}^{-1} \quad (43)$$

which are evaluated by Pople's point-charge approximation; and

$$\langle \phi_A^2(1) \left| \frac{1}{r_{12}} \right| \phi_A^2(2) \rangle = I_A + A_A \quad (44)$$

and

$$\langle \phi_B^2(1) \left| \frac{1}{r_{12}} \right| \phi_B^2(2) \rangle = I_B + A_B \quad (45)$$

which are evaluated by Pariser's approximations.

When Mulliken's approximation is applied to integral (35), a two-center, one-electron integral of the form

$$\langle \phi_B(2) | V_A(2) | \phi_B(2) \rangle \quad (46)$$

results, as well as a one-center, one-electron integral

$$\langle \phi_A(2) | V_A(2) | \phi_A(2) \rangle \quad (46a)$$

Integral (46) is evaluated by Pople's<sup>22</sup> point charge approximation whereas the one-center integral (46a) is evaluated analytically by approximating  $V_A$  as  $-Z_A/r$ . That is

$$\langle \phi_A(2) | V_A(2) | \phi_A(2) \rangle = -N^2 \int_0^\infty \int_0^\pi \int_0^{2\pi} r^{n^*-1} e^{-Z_{\text{eff}} r/n^*} \frac{Z_A}{r} r^{n^*-1} e^{-Z_{\text{eff}} r/n^*} r^2 \sin \theta d\theta d\phi dr, \quad (47)$$

where

$$N^2 = \frac{(2Z_{\text{eff}})^{2n^*+1}}{4(2n^*!)(n^*)^{2n^*+1}}$$

$Z_A$  is an adjustable parameter;  $r$  is the distance of the electron from the nucleus; and  $Z_{\text{eff}}$  and  $n^*$  are Slater parameters.

Evaluation of (47) yields

$$\langle \phi_A(2) | V_A(2) | \phi_A(2) \rangle = \frac{-Z_A Z_{\text{eff}}}{(n^*)^2} = \mu_A \quad (48)$$

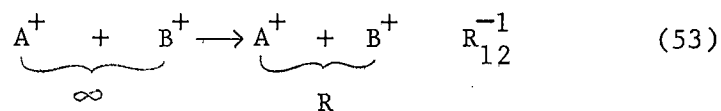
After expansion and evaluation of all the integrals,  $X_2$  may then be written as:

$$X_2 = \frac{-S_{AB}^2}{2} \left[ \mu_A + \mu_B + 2R_{12}^{-1} \right] - I_A S_{AB}^2 - I_B S_{AB}^2 + \frac{S_{AB}^2}{4} \left[ 2R_{12}^{-1} + I_A + I_B + A_A + A_B \right] \quad (49)$$

When  $X_1$  and  $X_2$  are incorporated,  ${}^3E_e$  is given as:

$$\begin{aligned}
 {}^3E_e = & \left[ \frac{1}{1 - S_{AB}^2} \right] \left[ -I_A - I_B - R_{12}^{-1} + S_{AB}^2 \{ I_A + I_B \right. \\
 & + \frac{M_A}{2} + \frac{\mu_B}{2} + R_{12}^{-1} \} - \frac{S_{AB}^2}{4} \{ I_A + I_B + A_A + A_B \\
 & \left. + 2R_{12}^{-1} \} \right] . \quad (50)
 \end{aligned}$$

By writing the electronic energy in this manner, all of the information needed may be found in tables. The electronic energy given by equation (50) represents the difference in energy of two positive ions, at the desired bond distance, and that of the neutral molecule at the same distance. Thus, to obtain the dissociation energy of the triplet state, three terms must be added to the electronic energy given by equation (50):



Equations (51) and (52) are simply producing ions from neutral molecules whose associated energies are the ionization potentials of A and B. Equation (53) represents the nuclear repulsion energy term involved in moving the two ions from infinity to distance R. This is



approximated as  $R_{12}^{-1}$ . With these additions, the total  ${}^3E$  is given as:

$${}^3E = {}^3E_e + I_A + I_B + R_{12}^{-1} . \quad (54)$$

With the evaluation of  ${}^3E$ , equation (12) then yields the coulombic and exchange integrals required by equation (10) to formulate the  $(H_2I_2)$  surface.

## CHAPTER IV

### RESULTS AND DISCUSSION

Before a potential surface can be constructed, certain constants must be evaluated. In the case of the empirical triplet state energy, equations (50) and (54), the ionization potentials and electron affinities are required. These quantities may be obtained from literature while  $\mu_{\text{H}}$  and  $\mu_{\text{I}}$  are calculated from Slater's constants using equation (48). For hydrogen, this yields  $\mu_{\text{H}} = -1$ . For iodine,  $\mu_{\text{I}} = -0.475 Z$  when Slater's  $Z_{\text{eff}}$  is taken as 7.6 and  $n^*$  as 4.0. In order to make the potential energy function fit the barrier height estimated from experimental activation energy data,  $Z$  is left as an adjustable parameter. The best fit is found for  $Z = 4.0$ . The required data for the calculation are given in Table I.

TABLE I  
CONSTANTS FOR CALCULATION OF  ${}^3\text{E}$

Atom	I(a.u.)	A(a.u.)
H	0.5000	-0.0276
I	0.4636	-0.1305

A comparison of data in Table II for  $H_2$  by this method using equation (54), and the data of Kolos and Roothaan<sup>19</sup> produces the following result:

$$\frac{{}^3E_T}{{}^3E_c} = 0.38871 \pm .02 \quad (55)$$

where  ${}^3E_T$  represents Kolos and Roothaan data and  ${}^3E_c$  represents data calculated by the empirical scheme described in Chapter III. The corrected  ${}^3E$  results for  $HI$  and  $I_2$  are therefore taken to be:

$${}^3E_T = 0.38871 {}^3E_c . \quad (56)$$

When equation (56) is applied to the  $HI$  and  $I_2$  systems, the data shown in Table III are obtained. Equation (16) can then be fitted by least-squares techniques to this data. This procedure produces the parameters  ${}^3D_e$  and  ${}^3$ .

These parameters, along with those for the singlet state of the system, are recorded in Table IV. This data, along with equations (13), (14), and (16) allow the coulomb and exchange integrals required by equation (10) to be calculated. Substitution of these values into that equation then produce the required potential surface.

The attributes of the surface represented by equation (10) can be illustrated through the use of contour maps. Such maps are shown in Figures (1)-(5).

TABLE II  
UNCORRECTED  ${}^3E_{H_2}$  FROM EQUATION (54)

R (a.u.)	${}^3E$ (e.V.)
1.00	20.02
1.20	17.63
1.40	14.48
1.60	11.59
1.80	9.22
2.00	7.31
2.20	5.79
2.40	4.60
2.60	3.63
3.20	1.76
4.00	0.64

TABLE III  
CORRECTED  $^3E$  FOR HI AND  $I_2$

R (a.u.)	$^3E_{HI}$ (e.V.)	R (a.u.)	$^3E_{I_2}$ (e.V.)
2.21	5.74	3.16	5.29
2.48	5.33	3.68	3.47
2.76	4.57	4.21	3.39
3.45	2.54	4.74	2.47
4.14	1.18	5.26	1.48
4.83	0.49	5.79	0.79
5.52	0.19	6.32	0.38
6.90	0.022	6.84	0.17

TABLE IV  
SINGLET AND TRIPLET STATE MORSE PARAMETERS

Parameter	$H_2$	$I_2$	HI
$^1D_e$ (e.V.)	4.7466	1.555	3.194
$^1\beta$	1.04435	0.9869	0.9468
$r_e$ (a.u.)	1.402	5.040	3.032
$^3D_e$ (e.V.)	1.9668	0.5741	1.1622
$^3\beta$	1.000122	0.4920	0.7335

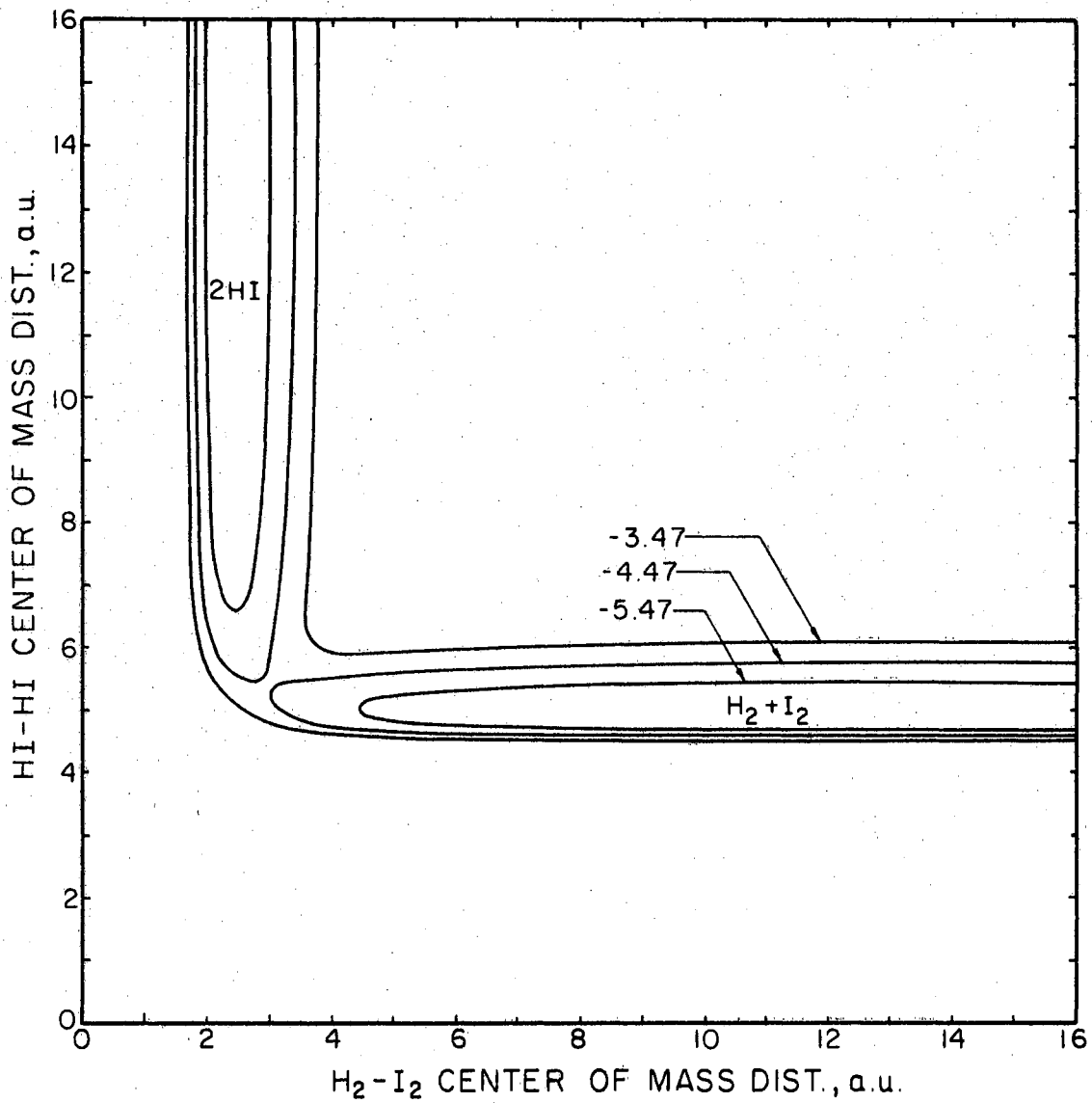


Figure 1. Regular, Planar Trapezoidal Configuration. (Energies in electron volts.)

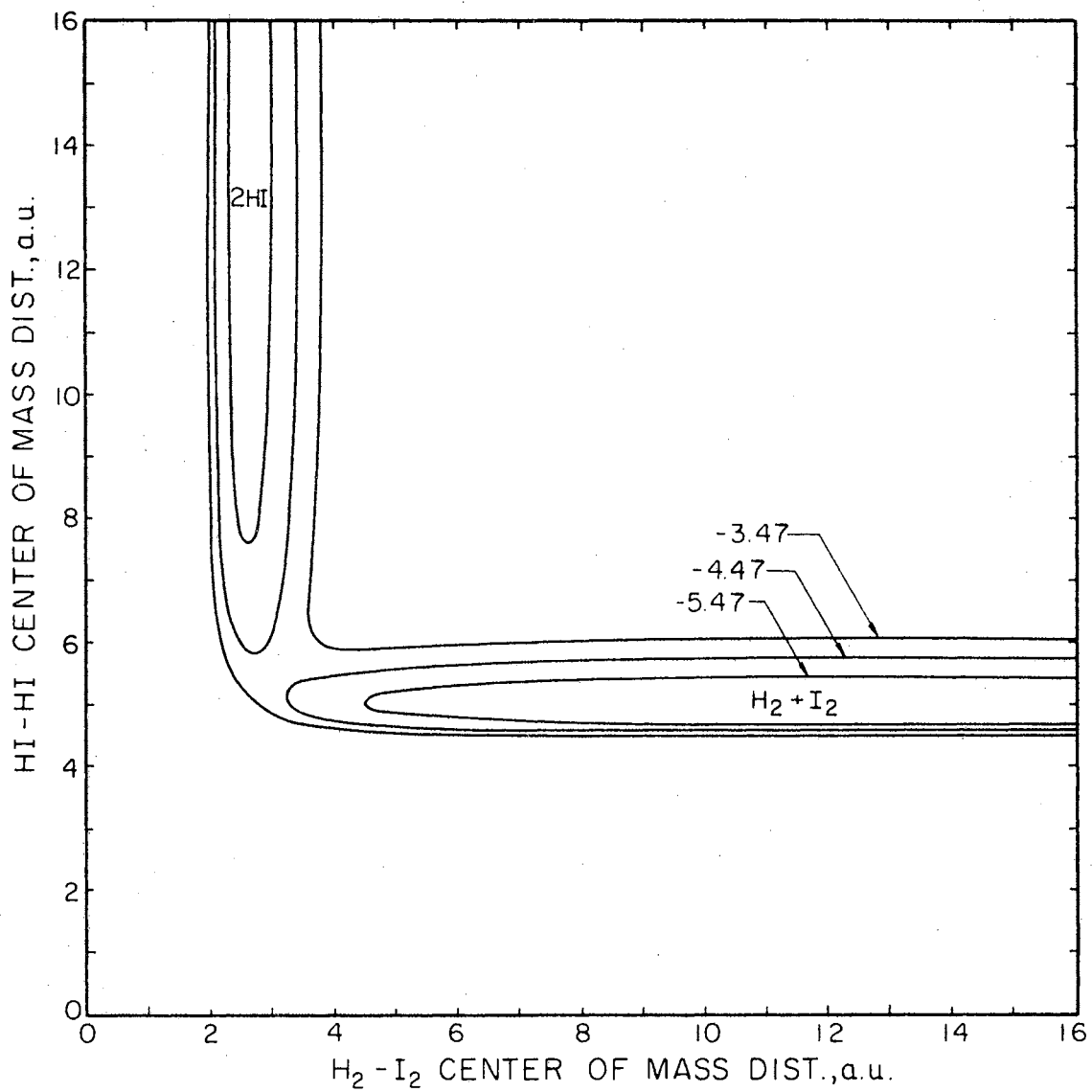


Figure 2. Distorted, Planar Trapezoidal Configuration. (Energies in electron volts.)

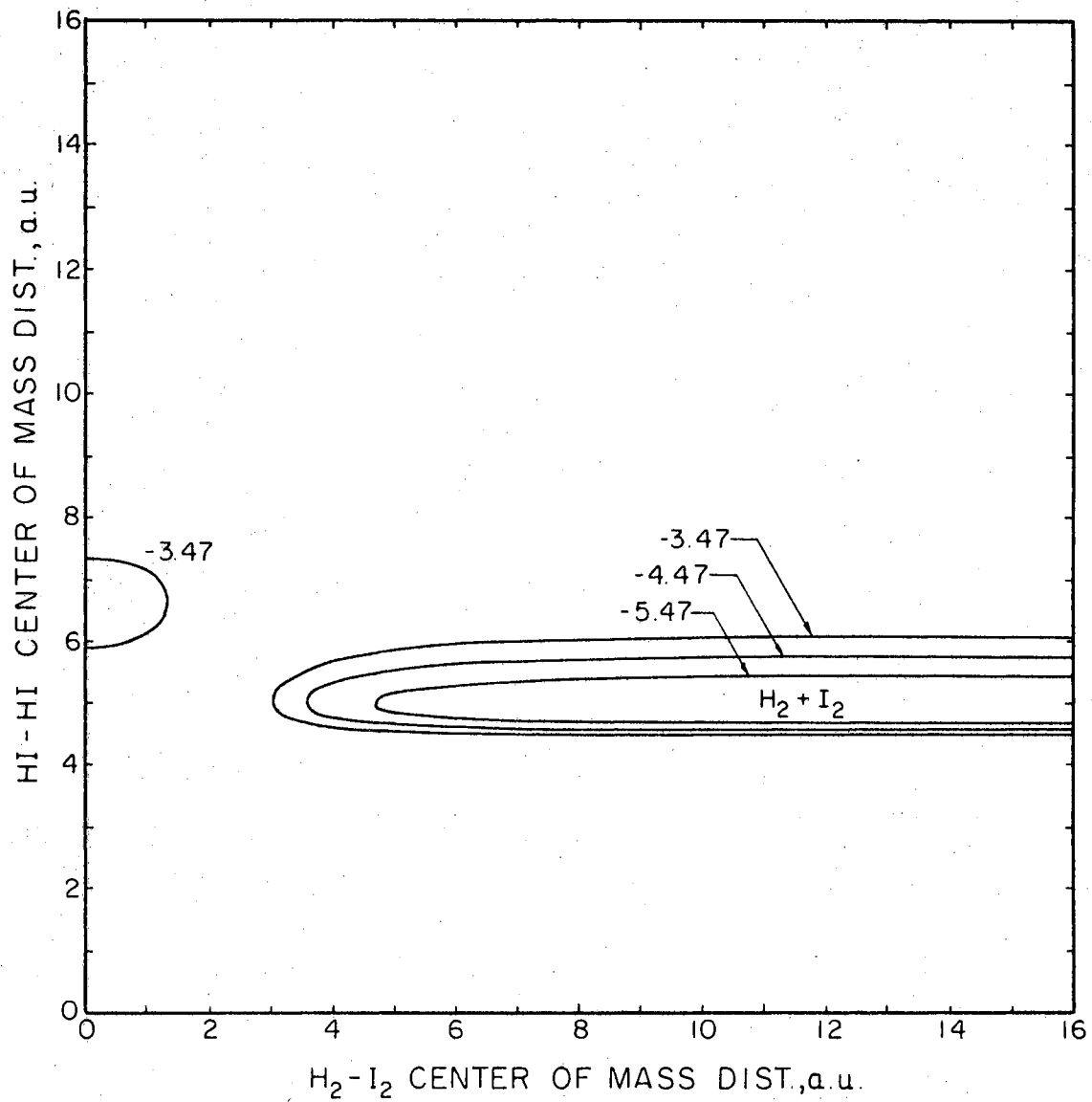


Figure 3. Out-Of-Plane Configuration. (Energies in electron volts.)



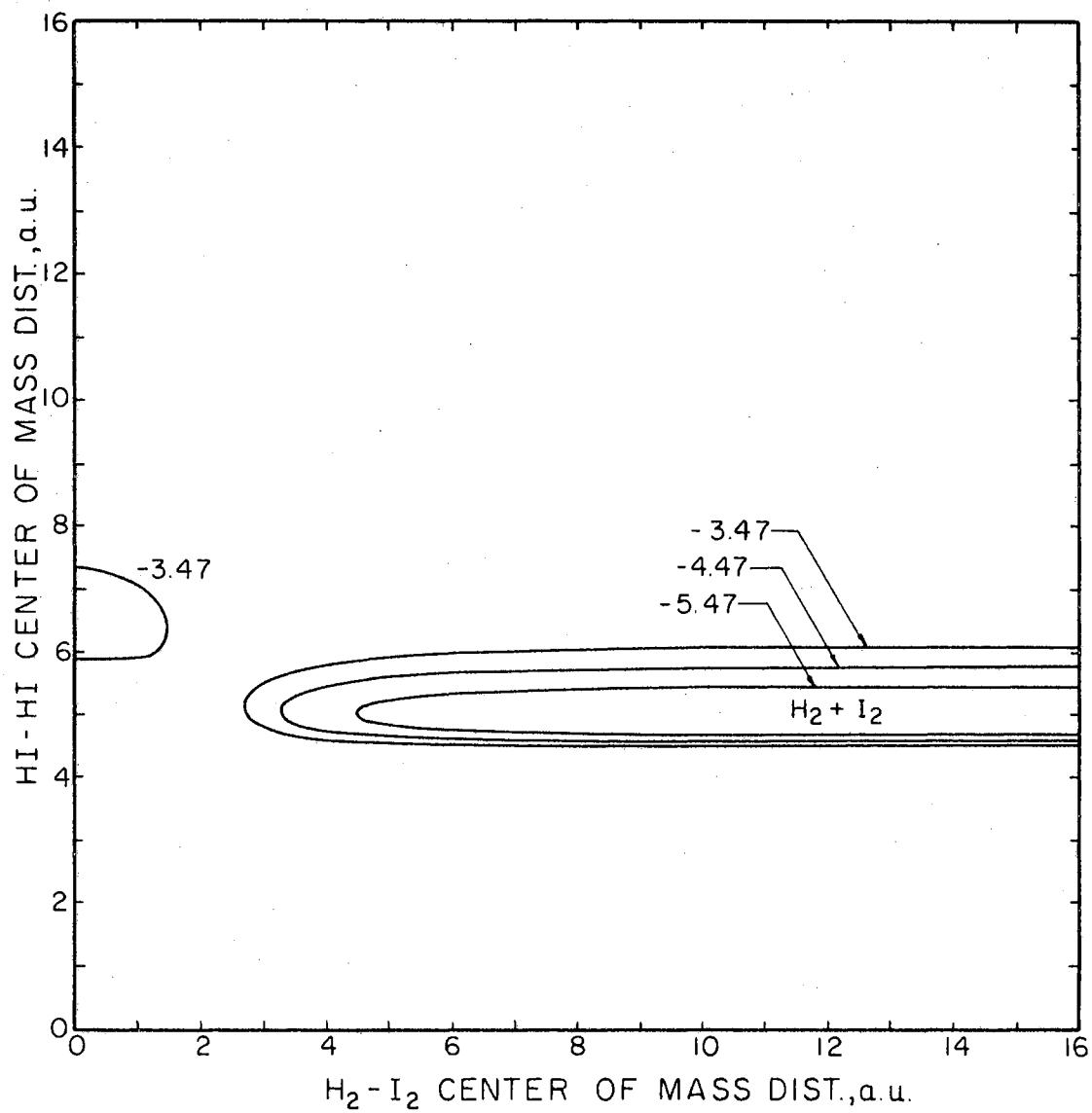


Figure 4. Perpendicular Configuration. (Energies in electron volts.)

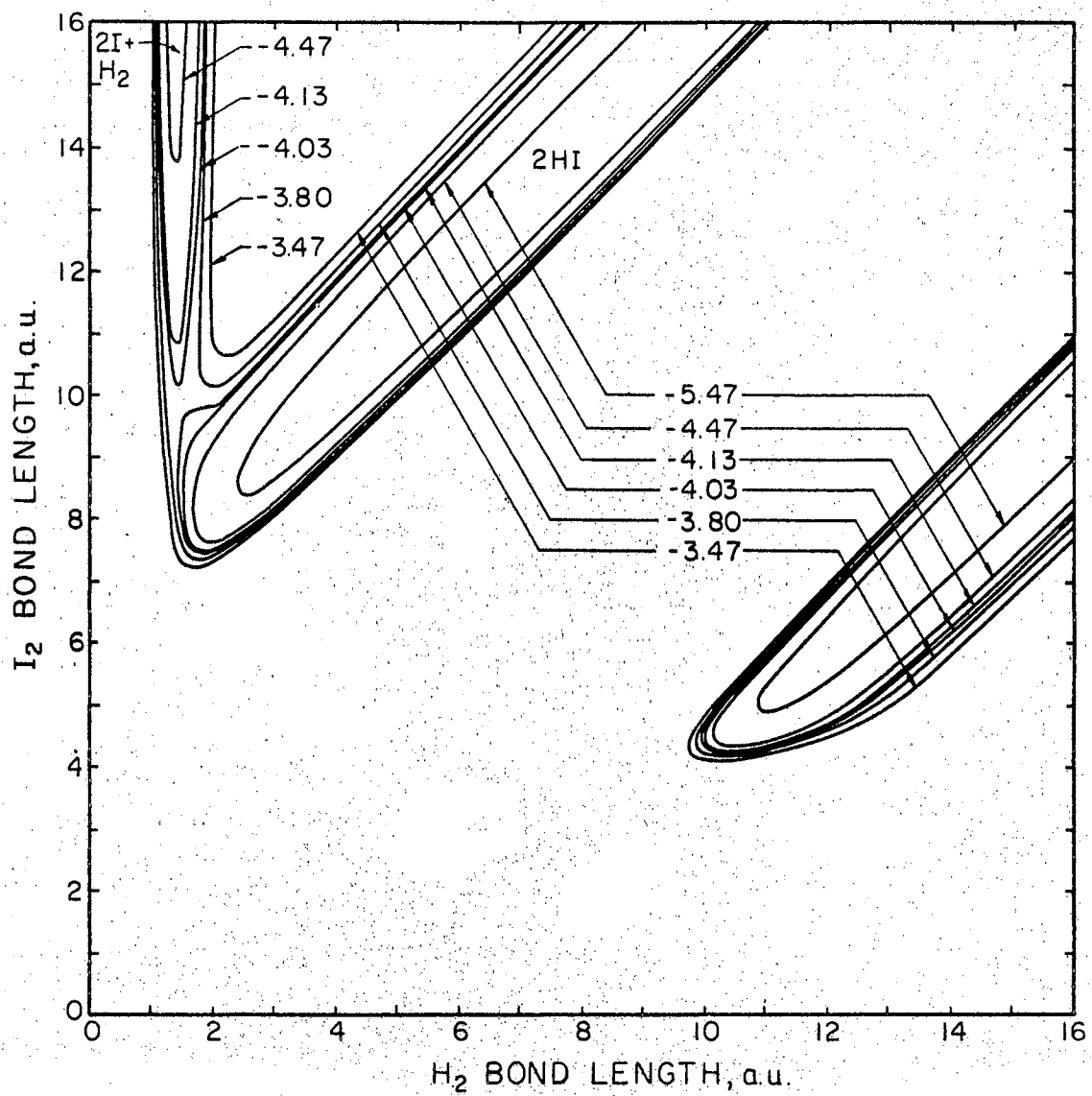


Figure 5. Linear Configuration. (Energies in electron volts.)

Figure (1) represents the regular, planar, trapezoidal configuration. In this configuration, the  $H_2$  bond is parallel to the  $I_2$  bond and the four nuclei are coplanar. For the contour maps of Figures (1)-(4), the  $I_2$  bond distance at all surface points is set equal to the sum of the  $H_2$  bond distance plus a constant. That constant is taken to be the difference between the  $I_2$  equilibrium bond length and the  $H_2$  equilibrium bond length. The variable coordinates of Figure (1) are the distances between the centers-of-mass of the two HI molecules and the distance between the centers-of-mass of the  $H_2$  and  $I_2$  molecules. By requiring that lines connecting these points be perpendicular, a regular trapezoid is formed with the  $I_2$  molecule as the base and the  $H_2$  molecule as the top.

If the distance between the centers-of-mass of the  $H_2$  and  $I_2$  molecules is large and the distance between the centers-of-mass of the two HI molecules is small, the system corresponds to the region at the lower right. This region would then represent an  $(H_2 + I_2)$  system. If the magnitudes of the distances were reversed, the upper left region would represent two HI molecules. By traveling from the lower right to the lower left and then to the upper left, the reaction coordinate for the reaction,  $H_2 + I_2 \rightarrow 2 HI$ , may be followed. The saddle-point for this surface occurs when the HI-HI center-of-mass distance and  $H_2$ - $I_2$  center-of-mass distance equal 5.4 a.u. and 3.0 a.u. respectively. The barrier for this reaction is calculated to be 1.83 electron volts.

A contour map for a distorted trapezoidal configuration is shown in Figure (2). This surface is formulated in the same manner as that of Figure (1) with one exception: the lines connecting the centers-of-mass of the two HI molecules and the centers-of-mass of the  $H_2$  and  $I_2$

molecules are not perpendicular. For Figure (1), the center-of-mass of the  $H_2$  molecule lies on the perpendicular bisector of the  $I_2$  bond axis. In Figure (2), the center-of-mass of  $H_2$  will be 0.5 atomic units off this perpendicular bisector. This has the effect of pushing the top of the trapezoid 0.5 atomic units to one side while holding the top and bottom parallel. The general form of the contour map in Figure (2) is the same as that shown in Figure (1). The barrier height on this contour map is 53 kcal. The saddle point is reached at the values of 5.6 a.u. for the HI-HI center-of-mass distance and 3.1 a.u. for the  $H_2$ - $I_2$  center-of-mass distance.

Figure (3) illustrates a non-planar surface in which the configuration represented by Figure (1) is altered by rotating the  $I_2$  molecule  $90^\circ$  out-of-plane. Although the complete reaction coordinate cannot be traced out on this surface, a comparison of energy contours for Figures (1) and (3) indicates that the expected reaction barrier along the out-of-plane path should be higher by perhaps as much as 1 electron volt.

Figure (4) represents a planar configuration in which the  $H_2$  molecule is pointed directly at the center-of-mass of the  $I_2$  molecule. This configuration is a "T" formation with  $I_2$  representing the brace and  $H_2$  lying on the stem. As the molecules move together, the  $H_2$  slides up the stem until one of the hydrogen atoms has passed between the iodine atoms forming a crossed structure. As can be seen, this surface is virtually identical to that shown in Figure (3).

For a linear configuration corresponding to the reaction of  $H_2 + 2I \rightarrow 2HI$  through a linear complex, one obtains a surface of the form shown in Figure (5). In this figure, the  $H_2$  and  $I_2$  centers-of-mass are superimposed with all four nuclei lying along a straight line. Energy

contour lines are plotted as a function of the  $H_2$  and  $I_2$  bond distances. The reaction coordinate for the above process begins at upper left with  $H_2 + 2I$ , then proceeds down to mid-left at the saddle point located at an  $I_2$  bond length of 10.0 a.u. and an  $H_2$  bond length of 1.5 a.u. At this point the barrier height relative to  $H_2 + I_2$  is 2.45 e.V. The reaction coordinate then continues to the right at a  $45^\circ$  angle to form 2 HI. When compared to the regular, planar, trapezoidal surface of Figure (1), the barrier height for reaction along a linear configuration appears to be about .44 e.V. higher.

## CHAPTER V

### SUMMARY AND CONCLUSIONS

Analysis of the five contour maps indicates that the lowest reaction barrier occurs with the regular trapezoidal configuration. In Figure (2), the distorted trapezoidal configuration raises the barrier slightly. The linear configuration shown in Figure (5) raises the barrier 0.44 electron volts. For the out-of-plane and perpendicular configurations, Figures (3) and (4), the barrier heights are quite high. The complex formed by the out-of-plane and perpendicular configurations appears to be too highly energetic to permit reaction to occur along that coordinate. The configuration that seems most favored for reaction is that of Figure (1), the regular trapezoidal configuration. For the reaction to proceed only by the termolecular mechanism would seem unlikely at this point. The termolecular mechanism appears to be a possible contributing mechanism but would certainly not appear to be the predominant one from analysis of the barrier heights of the contour maps. The experimental activation energy is reported<sup>3</sup> as 1.90 electron volts for the  $\text{H}_2 + \text{I}_2 \longrightarrow 2 \text{HI}$  reaction. The barrier height as taken from the regular trapezoidal configuration is 1.83 electron volts. This good agreement is not surprising since the parameter Z in the  $^3\text{E}$  calculations was adjusted to produce agreement of these values.

The above observations, based on barrier heights alone, are in apparent disagreement with experiment in that Sullivan's<sup>3</sup> results

indicate that a termolecular mechanism is responsible for the bulk of the reaction. This fact, in conjunction with the present work, would seem to indicate that the termolecular reaction path must be other than linear. Since a potential function for the  $(\text{H}_2\text{I}_2)$  system is available, classical trajectory studies of the reaction dynamics could now be carried out. Such calculations might answer some of these questions involved with the mechanisms. Although the potential energy surface is a semiempirical one, the general form is thought to be reasonable; the right diatomic energy limits are obtained and the barrier height is in excellent agreement with that reported experimentally.

#### BIBLIOGRAPHY

1. Bodenstein, M., Z. Physik. Chem., 29, 295 (1898).
2. Kistiakowsky, G. B., J. Am. Chem. Soc., 50, 2315 (1928).
3. Sullivan, J. H., J. Chem. Phys., 46, 73 (1967).
4. Noyes, R. M., J. Chem. Phys., 48, 323 (1968).
5. Glasstone, S., Laidler, K. J. and Eyring, H., The Theory of Rate Processes, McGraw-Hill, New York (1941).
6. Karplus, M., Porter, R. N. and Sharma, R., J. Chem. Phys., 40, 2033 (1964).
7. Sato, S., J. Chem. Phys., 23, 592 (1955).
8. Porter, R. N. and Karplus, M., J. Chem. Phys., 40, 1105 (1964).
9. Conroy, H. and Bruner, B. L., J. Chem. Phys., 47, 921 (1967).
10. Conroy, H., J. Chem. Phys., 41, 1327 (1964).
11. Conroy, H., J. Chem. Phys., 41, 1341 (1964).
12. Conroy, H., J. Chem. Phys., 41, 1331 (1964).
13. Conroy, H., J. Chem. Phys., 47, 912 (1967).
14. Conroy, H., J. Chem. Phys., 47, 930 (1967).
15. Karplus, M., Pederson, L. and Morokuma, K., J. Am. Chem. Soc., 89, 5064 (1967).
16. Heitler, W. and London F., Z. Physik, 44, 455 (1927).
17. London, F., Z. Elektrochem., 35, 552 (1929).
18. Morse, P., Phys. Rev., 34, 57 (1929).
19. Kolos, W. and Roothaan, C. C. J., Rev. Mod. Phys., 32, 219 (1960).
20. Pohl, H. A., Rein, R. and Appel, K., J. Chem. Phys., 41, 3385.
21. Pohl, H. A. and Raff, L. M., International Journal of Quantum Chemistry, 1, 577 (1967).



22. Pople, J. A., *Trans. Faraday Soc.*, 49, 1375 (1953).
23. Mulliken, R. S., *J. Chem. Phys.*, 46, 497 (1949).
24. Pariser, R. J., *Chem. Phys.*, 21, 568 (1953).

VITA

Lewis E. Stivers

Candidate for the Degree of  
Master of Science

Thesis: THEORETICAL INVESTIGATION OF THE  $(\text{H}_2\text{I}_2)$  POTENTIAL ENERGY SURFACE

Major Field: Chemistry

Biographical:

Personal Data: Born in Tulsa, Oklahoma, January 3, 1942, the son of Ralph and Grace Stivers.

Education: Graduated from Collinsville High School in 1960; received the Bachelor of Science degree in chemistry from University of Tulsa, Tulsa, Oklahoma, in 1965; completed requirements for Master of Science degree at Oklahoma State University in May, 1968.